energies

Article

Application of an NDIR Sensor System Developed for Early Thermal Runaway Warning of Automotive Batteries

Yulu Han [1,2,3,†], Yongmin Zhao [1,2,†], Anjie Ming [1,2,*], Yanyan Fang [4,*], Sheng Fang [4], Shansong Bi [4], Jiezhi Chen [5], Ran Xu [4], Feng Wei [1,2] and Changhui Mao [1,2]

1 State Key Laboratory of Advanced Materials for Smart Sensing, GRINM Group Co., Ltd., Beijing 100088, China
2 GRINM (Guangdong) Institute for Advanced Materials and Technology, Foshan 528000, China
3 General Research Institute for Nonferrous Metals, Beijing 100088, China
4 China Automotive Battery Research Institute Co., Ltd., Beijing 100088, China
5 School of Information Science and Engineering, Shandong University, Qingdao 266237, China
* Correspondence: mingaj@grinm.com (A.M.); fangyy@glabat.com (Y.F.)
† These authors contributed equally to this work.

Abstract: This paper proposes to apply a newly developed Non-Dispersive Infrared Spectroscopy (NDIR) gas sensing system composed of pyroelectric infrared detectors to monitor the thermal runaway (TR) process of lithium-ion batteries in real time and achieve an early warning system for the battery TR process. The new Electrical Vehicle Safety—Global Technical Regulation (EVS-GTR) requires that a warning be provided to passengers at least five minutes before a serious incident. The experimental results indicate that carbon dioxide and methane gas were detected during the overcharge test of the automotive battery, and the target gas was detected 25 s in advance before the battery TR when the battery vent was closed. In order to further explore the battery TR mechanism, an experiment was carried out using the battery sample with the battery vent opened. The target gas was detected about 580 s before the battery temperature reached the common alarm temperature (60 °C) of the battery management system (BMS). In this study, the beneficial effects of NDIR gas sensors in the field of thermal runaway warnings for automotive batteries were demonstrated and showed great application prospects and commercial value.

Keywords: automotive battery; thermal runaway; overcharge; NDIR gas sensor

check for updates

Citation: Han, Y.; Zhao, Y.; Ming, A.; Fang, Y.; Fang, S.; Bi, S.; Chen, J.; Xu, R.; Wei, F.; Mao, C. Application of an NDIR Sensor System Developed for Early Thermal Runaway Warning of Automotive Batteries. *Energies* **2023**, *16*, 3620. https://doi.org/10.3390/en16093620

Academic Editor: Gheorghe-Daniel Andreescu

Received: 3 March 2023
Revised: 7 April 2023
Accepted: 20 April 2023
Published: 22 April 2023

Copyright: © 2023 by the authors. Licensee MDPI, Basel, Switzerland. This article is an open access article distributed under the terms and conditions of the Creative Commons Attribution (CC BY) license (https://creativecommons.org/licenses/by/4.0/).

1. Introduction

Lithium-ion batteries (LIBs) have the advantages of high energy density and a long cycle life and are widely used in electric vehicles, hybrid electric vehicles, and power grids [1,2]. At present, the cathode materials for automotive lithium-ion batteries are mainly lithium iron phosphate (LiFePO4, LFP) and lithium cobalt manganate (LiCoxNiyMn1-x-yO2, NCM). Generally, lithium-ion batteries exhibit a certain thermal stability within their operating temperature range. In particular, LFP batteries are considered to be relatively safe cathode materials due to the high strength of the P-O bond in the phosphate radical of the cathode material. This bond is not easily broken at high temperatures [3,4].

However, in actual use, LIBs still present various forms and causes of failures. The most common on-site fault in the battery system of electric vehicles is overcharging, which is usually caused by failure of the battery management system (BMS) or charger and the inconsistency between batteries [1,5]. During overcharging, the positive electrode of a lithium-ion battery becomes excessively de-lithiated, while the negative electrode becomes excessively lithiated, resulting in a series of side reactions. [6,7]. Meanwhile, the insufficient thermal stability of the cathode material within the lithium-ion battery induces internal gas production, in addition to the TR risks caused by various gas production processes caused by the internal electricity and heat of the battery. According to the results of previous

studies, carbon dioxide (CO_2), methane (CH_4), and other gases are generated in the process of lithium-ion battery failure [8,9].

The excessive de-lithiation of lithium leads to the collapse of the cathode structure, accompanied by the generation of heat and the release of oxygen. The release of oxygen accelerates the oxidation and decomposition reactions of the electrolyte inside the lithium-ion battery, resulting in the rapid formation of a large amount of gas inside the battery. Since a lithium-ion battery is a hermetically sealed system, the internal pressure increases sharply in a short time, resulting in a more serious thermal runaway phenomenon, despite the good thermal stability of LFP. The heat released by these side reactions is the main factor that causes a lithium-ion battery to undergo a thermal runaway reaction, leading to fires and explosions [4]. Furthermore, this process usually involves the premature release of characteristic gases. Therefore, investigation of the gas production process is important for understanding the TR mechanisms of lithium-ion batteries and improving their safety performance.

Zhu et al. [10] conducted real-time measurements of battery voltage, current, and surface temperature during the overcharging process of a lithium-ion battery with a cathode material of NCM622 and a capacity of 30 Ah. The authors systematically studied the characteristics of an overcharge-induced battery thermal runaway and found that overcharge tests with high capacity rates (C-rates) are more dangerous than those with low C-rates. The peak value of the voltage curve increased linearly with the C-rates, but the temperature increase rate and the maximum surface temperature did not. The authors also found that a sharp drop in voltage always precedes the rapid rise in temperature before thermal runaway; thus, they proposed a safety monitoring signal based on voltage drops to warn users of the imminent risk of thermal runaway for batteries.

Gas production in normally operating lithium-ion batteries is primarily caused by electrolyte decomposition. Kong et al. [11,12] found that commercial batteries composed of lithium cobalt oxide (LCO), lithium manganate (LMO), and LFP produced the same gas components, which contained oxides such as CO_2 and CO, hydrocarbons such as C_2H_4 and CH_4, and gases such as H_2 [13]. The production of these gases was related to the reaction of electrolytes.

Generally, when the temperature reaches high temperatures of 80~120 °C, the negative solid electrolyte interface (SEI) film begins to decompose, and the gas production of the battery becomes significant. When the temperature reaches the melting temperature of the diaphragm (130~170 °C) [11,14], the battery will have a large-scale internal short circuit, and the heat will be released instantaneously, resulting in the release of active oxygen from the thermal decomposition of the positive electrode of cobalt-based batteries (such as NCM or NCA batteries), as well as the vaporization and redox reaction of the electrolyte.

The most advanced battery monitoring equipment in automotive battery packs uses Battery Management Systems (BMSs). BMSs are mainly used in electric vehicles for the intelligent management and maintenance of the battery pack and for monitoring the safety of the battery's status. The main functions of such systems are to ensure that each battery in the battery pack reaches a balanced and consistent state; accurately estimate the state of charge (SOC) of the power battery pack, that is, the remaining power of the battery; ensure that the SOC is maintained within a reasonable range; prevent damage to the battery due to overcharging; in the process of charging and discharging the battery, in real time, collect the terminal voltage and temperature, charging and discharging current, and total voltage of each battery in the battery pack; prevent overcharging or overdischarging of the battery; and simultaneously select problematic batteries to maintain the reliability and efficiency of the entire battery pack operation [15,16]. The BMS monitors the working status of the battery pack based on measurements from the temperature sensors, battery voltage, and current; estimates the SOC of the battery pack through algorithms; and maintains the reliability and efficiency of the entire battery pack operation.

New regulations such as GB 38031-2020 and the Electrical Vehicle Safety—Global Technical Regulation (EVS-GTR) dictate that passengers need to be alerted at least five

minutes before serious incidents occur [17,18]. In order to enhance the safety of batteries and satisfy EVS-GTR20 and GB 38031-2020, gas sensors are added to the battery pack based on BMS to detect the thermal runaway process of automotive batteries, thereby improving the safety of the batteries. BMS mainly detects changes in battery temperature, current and voltage, and impedance. Currently, research on the gas produced during the TR process of automotive batteries has mainly collected and analyzed the gas produced after the TR process. There is less research on monitoring gas production during the TR process. Currently, early thermal runaway warning systems have obvious limitations. (1) The vehicle automotive battery pack is composed of automotive batteries, and when a single battery has a thermal runaway phenomenon, the change is not significant. When BMS detects that the battery has a fault, the battery has often already begun an irreversible thermal runaway process. (2) The current means of improving the detection efficiency and accuracy of BMS systems is achieved through algorithm optimization, which cannot monitor the battery failure process in more dimensions. (3) The battery may fail even though the voltage does not change significantly, resulting in a failure to achieve a timely warning. In the early warnings of current BMS systems, individual batteries in the battery pack already experience irreversible thermal runaway before the alarm, meaning that such systems cannot meet the necessary safety requirements. For battery TR, the main detection gases that are produced include CO_2 and various combustible gases. The most commonly used gas sensors are divided into four categories, electrochemical sensors [9,14], semiconductor sensors [19–21], Non-Dispersive Infrared Spectroscopy (NDIR) gas sensors [22], and chemical sensors [23].

Cai et al. [24]. proposed a method for the early detection of the battery TR process by detecting CO_2 concentrations and demonstrated through COMSOL simulation that the gas sensor detection method can detect the TR process earlier. Koch et al. [25] designed a gas sensor system based on evaluating the impact of the TR process and proposed that designing a combination of multiple sensors for different batteries could eliminate the drawbacks of a single sensor and improve the reliability of the entire system. Christiane Essl et al. [9] tested several commercial gas sensors for four battery fault conditions. The research found that it is possible to use gas sensors for battery fault detection. The report mainly used metal oxide (MOx) gas sensors for detection, as such gas sensors can be used to detect the first venting event before TR in overheating and overcharging experiments. Based on this information, Ze Wang [26] described the metal oxide gas sensors used for battery thermal runaway.

Current research shows that applying gas sensors to detect the TR process in automotive batteries is more effective than detecting battery voltages and temperatures. Previous research mainly used MOx gas sensors and other types of gas sensors. NDIR gas sensors have the characteristics of low cost, high accuracy, and good stability—offering more accuracy than MOx gas sensors. NDIR gas sensors also have a longer working life and more stable performance than MOX gas sensors, as well as better selectivity for detecting gases. NDIR gas sensors are used in this study in the following ways: (1) to verify the feasibility of NDIR gas sensor TR process detection and (2) to make up for the shortcomings of other gas sensors by applying different sensor principles. We also plan to combine multiple sensors in subsequent research to form a commercially available sensor system for TR process monitoring. In this work, we developed an NDIR gas sensor based on a pyroelectric sensor with high accuracy and temperature stability. The NDIR gas sensor used in this work is based on our own previously developed high-performance pyroelectric infrared detector. This work applies the developed NDIR gas sensing system to monitor and analyze the gas production of lithium-ion batteries in real time. The gas sensing system can detect CO_2 and CH_4 during an overcharging test on LFP batteries and provide an early warning for the battery TR process.

2. Materials and Methods

2.1. Development of NDIR Gas Sensors

Pyroelectric infrared detectors are thermoelectric detectors that use pyroelectric materials with spontaneous polarization, such as lithium tantalate, $Pb(Zr11_xTi_x)O_3$(PZT), and triglycine sulfate(TGS), to detect infrared radiation. When a battery fails, the gas production process is often accompanied by high temperatures and explosions. Due to its optical principles, the NDIR gas sensing system can safely detect the gas production process. Previously, we reported a novel MEMS pyroelectric infrared detector based on a $LiTaO_3$ (LT) crystal with a highly absorptive amorphous carbon film layer [27].

Based on this technology, we developed an NDIR gas sensor system. NDIR gas sensors are widely used for measuring gas concentrations [28,29], IR breadth analysis [30,31] and environmental monitoring [32,33] via their molecular vibrations [34,35]. In this technology, an infrared beam passes through the sampling chamber, and each gas component in the sample absorbs infrared rays of a specific frequency, as shown in Figure 1. By measuring the change in specific infrared intensity received by the pyroelectric infrared sensor, the concentration change in the gas is obtained. The reason why this technology is non-dispersive is that the wavelength passing through the sampling cavity is not pre-filtered; instead, the optical filter is located in front of the detector and filters out all light except for the wavelength that the selected gas molecules can absorb. The infrared spectra of CO_2 and CH_4 are presented in Figure 2 [36]. For better gas detection resolution, a central wavelength with a higher absorption peak intensity is generally selected. It is also necessary to comprehensively consider avoiding water vapor interference and cross-interference from other gases. Taking the above factors into account, 4.26 and 3.31 μm were selected as the center wavelengths of the optical filters for the CO_2 and CH_4 sensors.

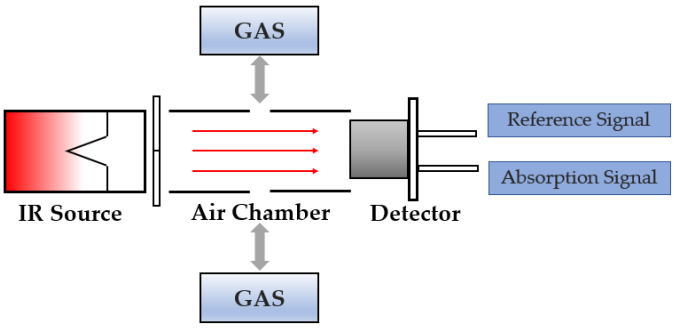


Figure 1. Structural diagram of the NDIR gas sensor.

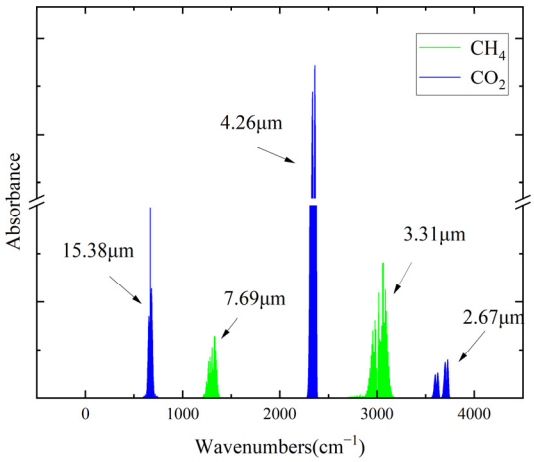


Figure 2. Infrared absorption bands of CO_2 and CH_4.

The circuit system uses an ARM microprocessor as the controller and includes a power management circuit, light source driving circuit, infrared light source, pyroelectric detector, secondary amplification and filtering circuit, signal acquisition circuit, and external interface. The ARM microprocessor uses an internal timer to generate a timing interrupt and controls the working state of the infrared light source and the sampling of the signal through timing. The output signal of the pyroelectric detector is a small current signal, which needs to be converted into a small voltage signal through a conversion circuit. The small voltage signal is amplified to the range that the microprocessor can recognize after passing through the amplification circuit. Finally, noise processing is performed on the amplified signal through an active filter circuit. An amplification filter circuit based on AD8617 for signal noise reduction, combined with a Kalman filter algorithm to achieve the accurate detection of gas concentration, is then designed and developed. The generated pyroelectric current is converted into the output voltage via the integrated circuit, and the output voltage is then measured using a lock-in amplifier, as shown in Figure 3.

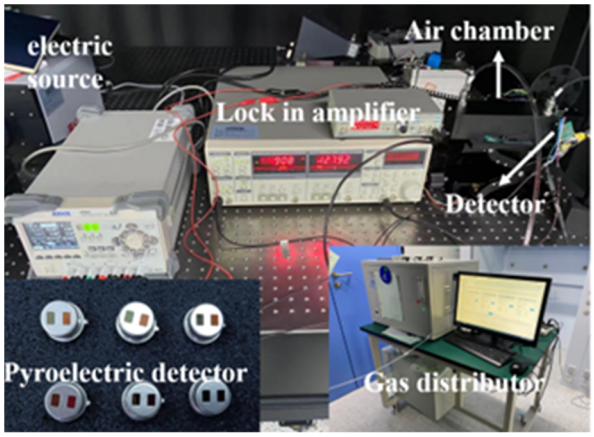


Figure 3. Site photo of the NDIR gas sensor test system.

We also need to convert the voltage value output by the pyroelectric detector into the gas concentration value. The infrared intensity of the measurement channel sensor decreases exponentially, as given by the Beer–Lambert equation [37]:

$$I = I_0 e^{-klx} \tag{1}$$

where coefficient k represents the effective absorption coefficient of gas, parameter I represents the light intensity after passing through the air chamber, parameter I_0 represents the incident light intensity, l represents the optical path length, and x represents the gas concentration. The change in light intensity can be expressed by the relative change in detector output voltage. Therefore, the relation of the gas concentration and voltage value output can be expressed as

$$x = -\frac{1}{kl}\ln\left(\frac{I}{I_0}\right) = -\frac{1}{kl}\ln\left(\frac{V}{V_0}\right) \tag{2}$$

2.2. NDIR Gas Sensor Performance Testing

CO_2 is used as an example to test the concentration of NDIR gas sensors with four different sensors and to verify whether the CO_2 measurement accuracy meets the technical requirements within the specified concentration range. As shown in Figure 4, the error between the respiratory rate test and the actual value of the four detectors is far less than the allowable error within the specified concentration range. When the concentration is at 15%, the maximum deviation is 1.75, and the maximum actual error is less than 4%. When the concentration is lower than 10%, the error of the four detectors is about 1%, and

the repeatability is good. Thus, the detectors meet the technical requirements for precise CO_2 measurements.

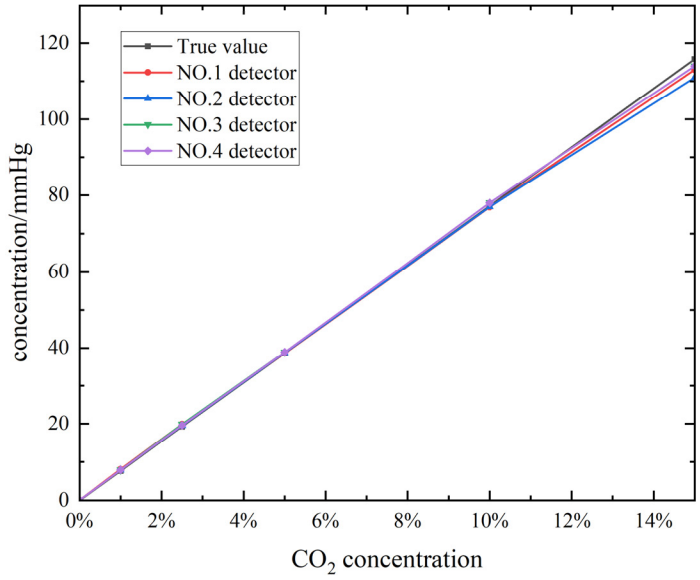


Figure 4. CO_2 accuracy verification of NDIR gas sensors.

Furthermore, NDIR gas sensors are susceptible to temperature drift, as a significant amount of heat is generated during the overcharge failure testing of automotive batteries, including ohmic heat and reaction heat, which can cause the ambient temperature to rise. After algorithmic correction, we tested the temperature stability of four different sensors. As shown in Figure 5, the output signals of the CO_2 channels and the reference channels of the four detectors increased with an increase in temperature, with change rates of 4%, 3.8%, 4.1%, and 4.1%, respectively, which conforms to the rule that pyroelectric materials are affected by temperature. The detector law has a good repeatability, and the temperature compensation corrections were performed using the module algorithm to meet the application requirements.

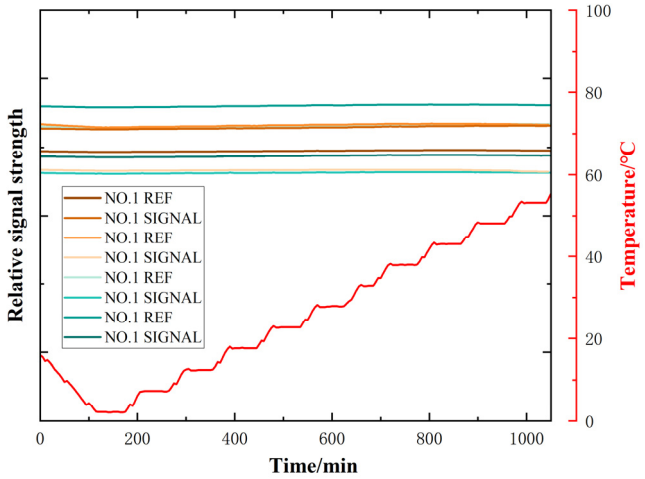
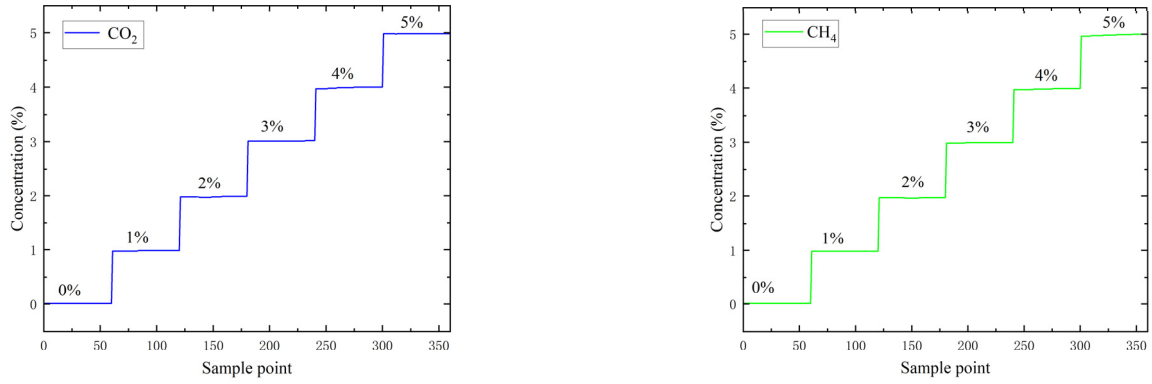


Figure 5. NDIR gas sensor temperature stability test.

The NDIR sensor used in the experiment was tested for the accuracy of gas concentration using 5% standard gas and a 1% gradient. The test results are shown in Figure 6. The maximum change of the detector was 0.02%. The NDIR module we developed has high accuracy, and the designed range is very suitable for battery failure gas production

experiments. Since NDIR gas sensors are optical sensors, various gases and substances generated during battery failure will not affect the sensor.



(**a**) (**b**)

Figure 6. NDIR sensor gas concentration test: (**a**) CO_2; (**b**) CH_4.

3. Experiments

In this experiment, we designed an explosion-proof testing room. The system was installed in an explosion-proof test room due to the possibility of heating and even explosion during the battery overcharge test. Meanwhile, during the failure process of the battery, various types of electrolyte vapors were generated, so the experiment was conducted in a closed environment. Firstly, the chamber was vacuumed and filled with nitrogen to a normal pressure in order to eliminate interference from other gases. The experimental system diagram is shown in Figure 7. In this study, 50 Ah commercial LIBs with lithium iron phosphate cathodes were used for the overcharging experiment. The main performance parameters of the battery are shown in Table 1. The gas detector was fixed 12 cm above the battery explosion vent, as shown in Figure 7. The CO_2 sensor range was 0~20%, and the CH_4 sensor range was 0~5%.

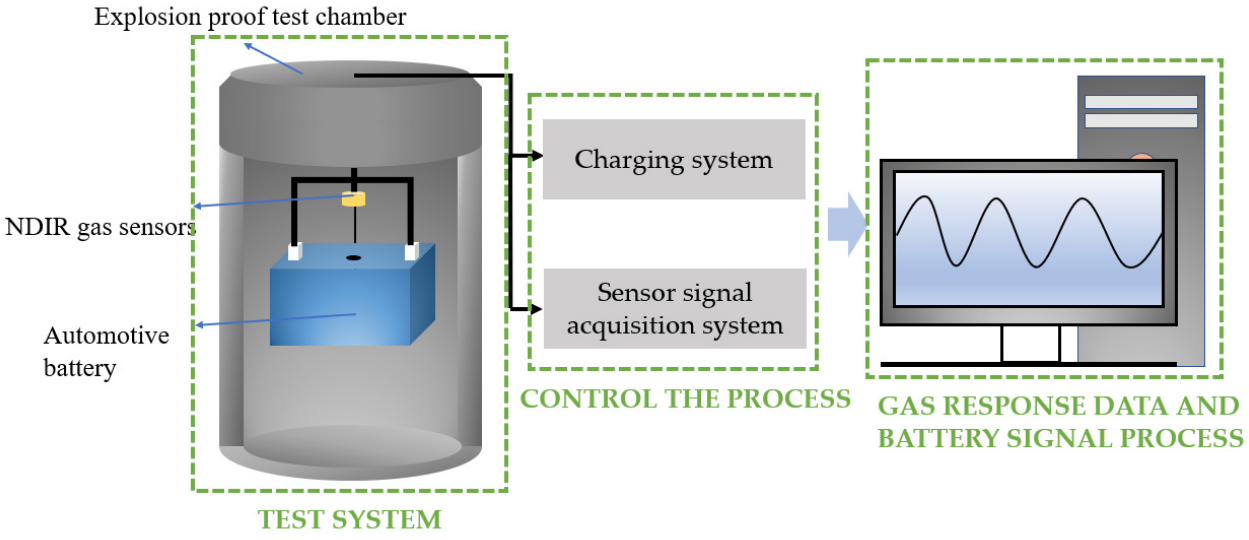


Figure 7. Structural diagram of the battery TR test.

Table 1. Performance parameters of the lithium-ion automotive battery for the experiment.

Type	LFP Battery
Chemical composition	positive pole: LFP negative pole: LiC_6
Rated capacity	50 Ah
Size	147 × 115 × 28 mm
Mass	986 g
Standard voltage	3.0 V

After setting up the test system, the experimental steps taken were as follows. (1) First, the lithium-ion automotive battery was left to stand for 10 min to stabilize the voltage and current and preheat the gas sensor. (2) Then, we used a 50 A constant current to overcharge the automotive battery. When the voltage increased rapidly, a thermal runaway was considered to occur; then, we stopped the overcharging and moved to the static step. (3) The static battery was used to continuously record the voltage change, the gas sensor collected the gas concentration change, and the data acquisition equipment collected the temperature fluctuation at each thermocouple monitoring point on the surface of the automotive battery.

For this experiment, six temperature monitoring points were established by attaching thermocouples. These monitoring points are indicated in Figure 8, and the position settings are shown in Table 2. By comparing and analyzing the temperature changes of these six temperature detection points, the corresponding temperature trends of lithium-ion power batteries with overcharging-induced thermal runaway behavior were relatively accurately obtained, allowing us to better analyze the internal mechanisms of battery overcharging thermal runaways.

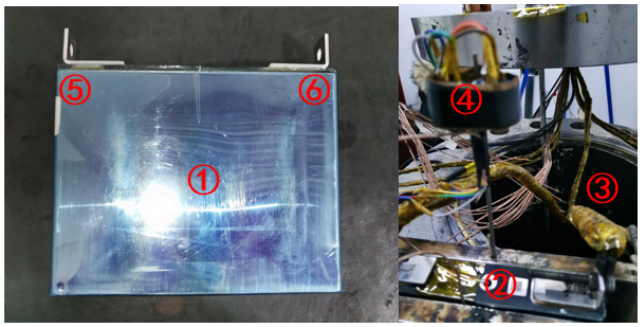


Figure 8. Distribution of the temperature monitoring points.

Table 2. Thermopile sensor set points.

Thermopile Sensors	Position Settings
1	The center of the battery surface
2	The battery explosion vent
3	The ambient temperature
4	The gas sensor
5	The positive poles of the battery
6	The negative poles of the battery

4. Results and Discussion

In the first experiment, the preliminary feasibility of using NDIR gas sensors to detect gas production in automotive battery failures was verified without opening the automotive battery explosion vent. Figure 9a shows the temperature variation at different points during the overcharging experiment. A significant amount of heat was generated during the battery TR, mainly concentrated in the positive electrode and the center of

the battery. In Figure 9a, it can be seen that, as the overcharging reaction of the battery progressed, the overall temperature of the battery gradually increased. At about 1600 s, there was a significant decrease in the temperature of the battery's negative electrode and the temperature of the battery vent, indicating that a large amount of gas had accumulated inside the battery, reaching the critical value for the vent to open. With the opening of the vent, the release of a large amount of gas carried away some of the heat, causing a decrease in the temperature of the vent. The position of the sensor and the ambient temperature change in the explosion-proof test chamber were within the correction range of the NDIR gas sensor algorithm (less than 80 °C), and the influence of temperature on the concentration change in the detector could be excluded.

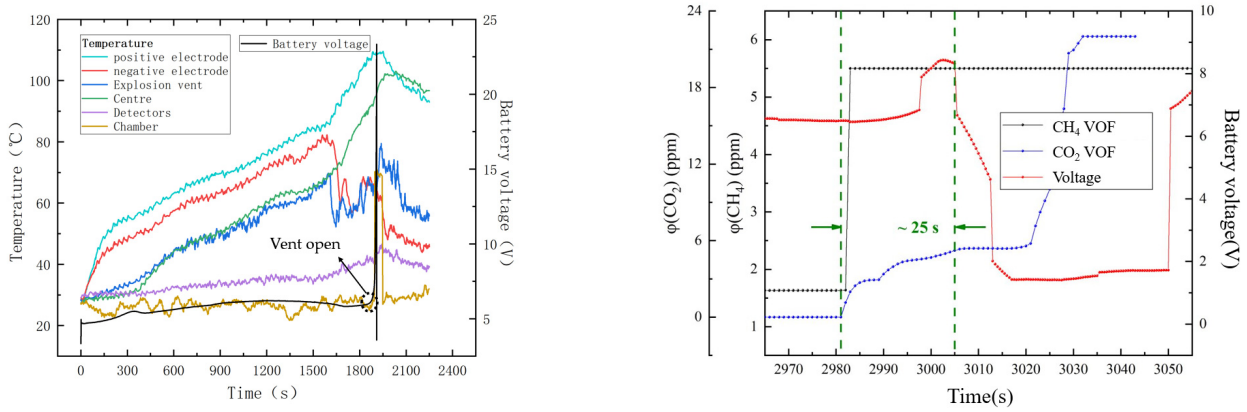


Figure 9. (**a**) During battery overcharging, the battery temperature, chamber temperature, and detector ambient temperature changed; (**b**) in the overcharging experiment, the battery voltage and the concentration of CO_2 and CH_4 changes. The concentration change time was 25 s ahead of the voltage change time.

Figure 9b shows the changes in gas concentration and battery voltage. In the battery failure experiment, a dramatic change in the positive voltage indicated that the battery had begun to fail. A sharp drop in voltage meant that the explosion vent had opened. As shown in Figure 9b, the battery voltage dropped sharply after a sharp increase in CO_2 and CH_4 concentrations for 25 s, demonstrating that the developed NDIR gas sensor enabled the early detection of battery failure.

We observed that a large amount of gas accumulated in the battery when the explosion vent of the automotive battery was not opened. When the battery voltage increased sharply, the battery experienced a thermal runaway effect, and the explosion vent was blown away by a large amount of gas. At this time, the sensors were positioned facing the explosion vent, resulting in a sharp increase in gas concentration that quickly exceeded the sensor's range. As shown in Figure 9, CH_4 gas reached its full scale after the explosion vent was opened, and the large amount of CO_2 generated as a reaction by-product was oxidized.

Although the application of NDIR gas sensors in the battery TR process was preliminarily verified in the first experiment, the timing of gas signal testing by the sensors was not much earlier than that of the voltage testing in the experiment. At the same time, as a large amount of gas was generated beyond the range of the sensor, it became impossible to accurately measure the ratio of gas production and gas composition during the TR process. After the battery overcharging experiment, the gas sensor that was stimulated by high-temperature gas malfunctioned and could not function properly.

In the second experiment, to comprehensively detect the gas production during automotive battery failure, the vent of the automotive battery was opened, and the experiment was repeated. After opening the vent, the gas generated by the battery during the TR process did not accumulate in the battery, preventing the generation of a large amount of

gas from exceeding the range of the gas sensor. At the same time, the gas concentrations generated at different stages of the TR process were also more clearly detected. However, the temperature and voltage changes caused by the overcharging of the lithium-ion automotive battery were uncontrollable, as shown in Figure 10.

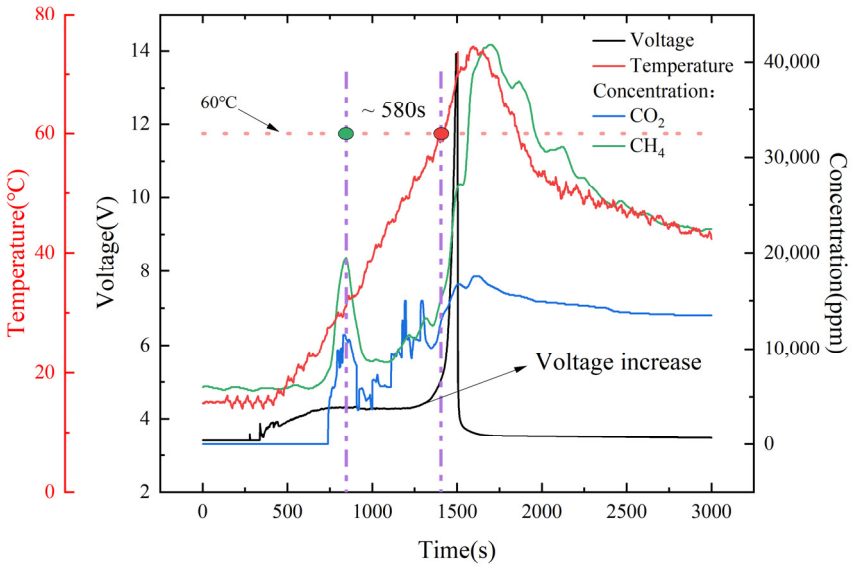
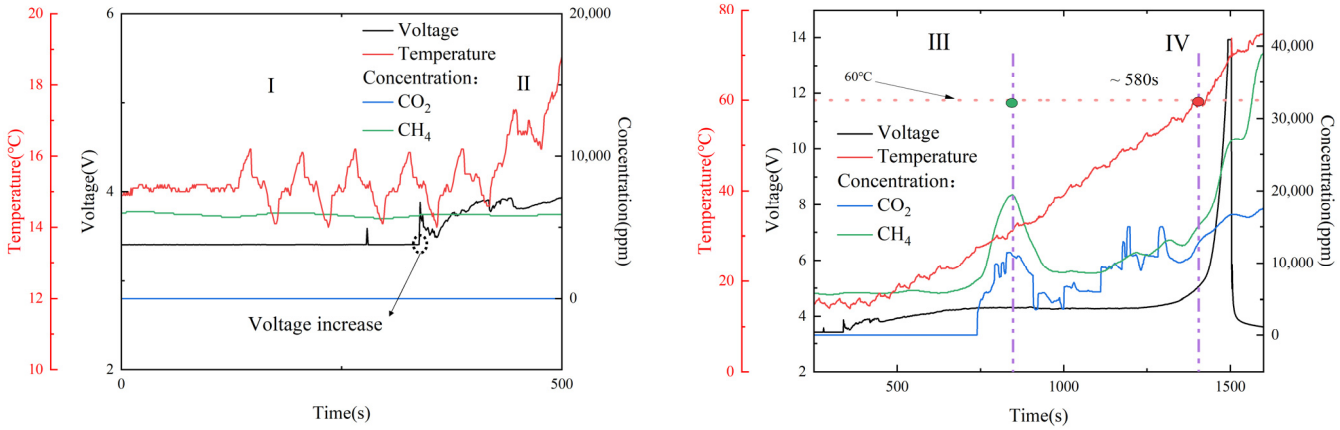


Figure 10. Change in temperature, voltage, and gas concentration during overcharging.

According to the temperature and voltage change characteristics, the voltage curve for the whole process of overcharging and runaway can be divided into four stages.

In the first stage (I), the lithium-ion automotive battery's initial charging voltage was 3.4 V, and after 338 s of continuous overcharging to the first voltage inflection point, the battery temperature slowly started to rise, with there being no obvious change in the gas sensor, as shown in Figure 11a.



(**a**) (**b**)

Figure 11. (**a**) The first and second stage changes in temperature, voltage, and gas concentration during overcharging; (**b**) the third and fourth stage changes of temperature, voltage, and gas concentration during overcharging.

In the second stage (II), 400 s after the first voltage inflection point, the automotive battery voltage gradually increased to 4.3 V, and the CO_2 and CH_4 gas sensors detected the generation of gas and produced a peak value at the same time, which demonstrated that

the automotive battery started to fail at this time, as shown in Figure 11b. The temperature then increased from 15 to 31.8 °C, with a temperature rise rate of 2.52 °C/min.

In the third stage (III), the automotive battery voltage appeared as a voltage plateau period. The voltage plateau represents the external manifestation of the coexistence of multiple phase states in the internal chemical reaction of the lithium-ion automotive battery, indicating that, at this stage, the lithium ion in the lithium salt was converted to a new relatively stable stage and new substances were beginning to form. The temperature gradually increased from 31.8 to 60 °C, and the temperature increase rate slightly rose to 2.91 °C/min. When the temperature reached 60 °C, the battery management system's alarm temperature was reached. The concentration of gas produced by the battery also gradually increased. The time from the first peak value collected by the gas sensor to the battery alarm was about 580 s faster than expected, which has a certain significance for battery safety warnings.

In the fourth stage (IV), the temperature of the lithium-ion automotive battery continued to rise, further accelerating the decomposition and exothermic reaction of the positive and negative active materials and the electrolyte. The generation of a large amount of gas in the battery led to a rapid increase in internal resistance, and the voltage increased rapidly to 14 V, causing irreversible thermal loss of control in the automotive battery. The gas production concentration then reached the maximum value.

After the battery experienced thermal runaway and stopped overcharging, the internal energy of the automotive battery began to dissipate, causing the temperature to drop. Additionally, the gas concentration also began to decrease, and the reaction gradually ceased.

In order to meet the new regulations of GB 38031-2020 and EVS-GTR and warn passengers at least five minutes before a serious accident occurs, in this experiment, after opening the venting port, when the gas sensor detected a signal, that signal was compared to the battery temperature reaching the BMS system alarm temperature of 60 °C, which was increased by ~580 s. Compared to Christiane Essl's research results [9], this experiment design significantly advanced the warning of battery TR process.

However, the NDIR gas sensor still has some issues: (1) Hydrogen gas is also produced in large quantities during the battery failure process, but NDIR gas sensors cannot selectively detect hydrogen gas because hydrogen gas does not have an infrared characteristic peak. (2) NDIR gas sensors are more expensive than MOx gas sensors. (3) Since NDIR gas sensors are optical sensors, they require a light source and an optical path, creating the demand for a larger volume. To solve these three problems, we could combine multiple sensors to achieve the high precision, low cost, simultaneous detection of multiple gases to improve the reliability of monitoring in future research on monitoring the battery failure process. Going forward, gas sensors could be integrated into the automotive battery to reduce volume. At the same time, the structure of NDIR gas sensors could be further optimized to reduce cost and size.

5. Conclusions

This study presents a novel method for detecting battery failure by monitoring the changes in gas concentration generated during the failure process. An NDIR gas sensor was used to detect the battery TR process, and its feasibility was verified. The system utilized a high-performance pyroelectric detector along with a newly designed circuit system and noise reduction algorithm. In tests using CO_2 and CH_4, we were able to detect the target gas 25 s before the battery failed completely, when the explosion vent of the automotive battery was not opened. Upon opening the explosion vent of the automotive battery, we were able to detect the target gas approximately 580 s before the BMS alarm and then analyze the gas generation process of lithium iron phosphate automotive battery overcharging failure. As the system is continuously improved, the warning time will be extended to include battery safety warning functionality.

Author Contributions: Conceptualization, A.M. and Y.F.; methodology, Y.Z. and S.F.; validation, Y.H. and S.B.; investigation, Y.H., S.B., and Y.Z.; resources, S.F. and F.W.; data curation, J.C.; writing—original draft preparation, Y.H.; writing—review and editing, A.M. and Y.F.; supervision, C.M. and R.X.; administration, A.M. and J.C. All authors have read and agreed to the published version of the manuscript.

Funding: This research was funded by the National Natural Science Foundation of China (No. 61874137), Beijing Gold–Bridge Project (No. ZZ19029), Shandong Provincial Key Research and Development Program (No. 2020CXGC010203), Key R & D project of Guangdong Province (Grant No. 2021B0909060001).

Data Availability Statement: Not applicable.

Conflicts of Interest: The authors declare no conflict of interest.

References

1. Huang, W.; Feng, X.; Han, X.; Zhang, W.; Jiang, F. Questions and Answers Relating to Lithium-Ion Battery Safety Issues. *Cell Rep. Phys. Sci.* **2021**, *2*, 100285. [CrossRef]
2. Zaghib, K.; Dubé, J.; Dallaire, A.; Galoustov, K.; Guerfi, A.; Ramanathan, M.; Benmayza, A.; Prakash, J.; Mauger, A.; Julien, C.M. Enhanced thermal safety and high power performance of carbon-coated $LiFePO_4$ olivine cathode for Li-ion batteries. *J. Power Sources* **2012**, *219*, 36–44. [CrossRef]
3. Wen, J.; Yu, Y.; Chen, C. A Review on Lithium-Ion Batteries Safety Issues: Existing Problems and Possible Solutions. *Mater. Express* **2012**, *2*, 197–212. [CrossRef]
4. Doh, C.H.; Kim, D.H.; Kim, H.S.; Shin, H.M.; Jeong, Y.D.; Moon, S.I.; Jin, B.S.; Eom, S.W.; Kim, H.S.; Kim, K.W.; et al. Thermal and electrochemical behaviour of C/Li_xCoO_2 cell during safety test. *J. Power Sources* **2008**, *175*, 881–885. [CrossRef]
5. Zeng, Y.; Wu, K.; Wang, D.; Wang, Z.; Chen, L. Overcharge investigation of lithium-ion polymer batteries. *J. Power Sources* **2006**, *160*, 1302–1307. [CrossRef]
6. Chen, S.; Wang, Z.; Yan, W. Identification and characteristic analysis of powder ejected from a lithium ion battery during thermal runaway at elevated temperatures. *J. Hazard. Mater.* **2020**, *400*, 123169. [CrossRef] [PubMed]
7. Beletskii, E.V.; Fedorova, A.A.; Lukyanov, D.A.; Kalnin, A.Y.; Ershov, V.A.; Danilov, S.E.; Spiridonova, D.V.; Alekseeva, E.V.; Levin, O.V. Switchable resistance conducting-polymer layer for Li-ion battery overcharge protection. *J. Power Sources* **2021**, *490*, 229548.1–229548.10. [CrossRef]
8. Kumai, K.; Miyashiro, H.; Kobayashi, Y.; Takei, K.; Ishikawa, R. Gas generation mechanism due to electrolyte decomposition in commercial lithium-ion cell. *J. Power Sources* **1999**, *81–82*, 715–719. [CrossRef]
9. Essl, C.; Seifert, L.; Rabe, M.; Fuchs, A. Early Detection of Failing Automotive Batteries Using Gas Sensors. *Batteries* **2021**, *7*, 25. [CrossRef]
10. Zhu, X.; Wang, Z.; Wang, Y.; Wang, H.; Wang, C.; Tong, L.; Yi, M. Overcharge investigation of large format lithium-ion pouch cells with $Li(Ni_{0.6}Co_{0.2}Mn_{0.2})O_2$ cathode for electric vehicles: Thermal runaway features and safety management method. *Energy* **2019**, *169*, 868–880. [CrossRef]
11. Kong, W.; Li, H.; Huang, X.; Chen, L. Gas evolution behaviors for several cathode materials in lithium-ion batteries. *J. Power Sources* **2005**, *142*, 285–291. [CrossRef]
12. Galushkin, N.E.; Yazvinskaya, N.N. Echanism of Gases Generation during Lithium-Ion Batteries Cycling. *J. Electrochem. Soc.* **2019**, *166*, A897–A908. [CrossRef]
13. Yu, Y.; Lee, S.J.; Theerthagiri, J.; Lee, Y.; Choi, M.Y. Architecting the AuPt alloys for hydrazine oxidation as an anolyte in fuel cell: Comparative analysis of hydrazine splitting and water splitting for energy-saving H_2 generation. *Appl. Catal. B Environ.* **2022**, *316*, 121603. [CrossRef]
14. Pinnangudi, B.N.; Dalal, S.B.; Medora, N.K.; Arora, A.; Swart, J. Thermal shutdown characteristics of insulating materials used in lithium ion batteries. In Proceedings of the 2010 IEEE Symposium on Product Compliance Engineering Proceedings, Boston, MA, USA, 18–20 October 2010; pp. 1–5.
15. Rahimi-Eichi, H.; Ojha, U.; Baronti, F.; Chow, M.Y. Battery management system: An overview of its application in the smart grid and electric vehicles. *IEEE Ind. Electron. Mag.* **2013**, *7*, 4–16. [CrossRef]
16. Liu, K.; Li, K.; Peng, Q.; Zhang, C. A brief review on key technologies in the battery management system of electric vehicles. *Front. Mech. Eng.* **2019**, *14*, 47–64. [CrossRef]
17. *GB 38031-2020*; National Standard of the People's Republic China (GB): Electric Vehicles Traction Battery Safety Requirements. Standardization Administration: Beijing, China, 2020; pp. 1–42.
18. Kenichiroh, K. Journey to a New Regulatory Option. In *OICA Submission to IWG for GTR 20, Phase 2*; United Nations Economic Commission for Europe (UNECE): Berlin, Germany, 2019.
19. Das, S.; Jayaraman, V. SnO_2: A comprehensive review on structures and gas sensors. *Prog. Mater. Sci.* **2014**, *66*, 112–255. [CrossRef]
20. Chaudhary, S.; Umar, A.; Bhasi, K.; Baskoutas, S. Chemical Sensing Applications of ZnO Nanomaterials. *Materials* **2018**, *11*, 287. [CrossRef] [PubMed]

21. Tamvakos, A.; Calestani, D.; Tamvakos, D.; Pullini, D.; Sgroi, M.; Pruna, A. Low concentration CO gas sensing properties of hybrid ZnO architecture. *Microelectron. Eng.* **2016**, *160*, 12–17. [CrossRef]
22. Gibson, D.; MacGregor, C. A Novel Solid State Non-Dispersive Infrared CO_2 Gas Sensor Compatible with Wireless and Portable Deployment. *Sensors* **2013**, *13*, 7079–7103. [CrossRef]
23. Zhou, R.; Vaihinger, S.; Geckeler, K.; Göpel, W. Reliable CO_2 sensors with silicon-based polymers on quartz microbalancetransducers. *Sens. Actuat. B Chem.* **1994**, *19*, 415–420. [CrossRef]
24. Cai, T.; Stefanopoulou, A.G.; Siegel, J.B. Early Detection for Li-Ion Batteries Thermal Runaway Based on Gas Sensing Ting. *ECS Trans.* **2019**, *89*, 85–97. [CrossRef]
25. Koch, S.; Birke, K.P.; Kuhn, R. Fast thermal runaway detection for lithium-ion cells in large scale traction batteries. *Batteries* **2018**, *4*, 16. [CrossRef]
26. Wang, Z.; Zhu, L.; Liu, J.; Wang, J.; Yan, W. Gas Sensing Technology for the Detection and Early Warning of Battery Thermal Runaway: A Review. *Energy Fuels* **2022**, *36*, 6038–6057. [CrossRef]
27. Sun, X.; Ming, A.; Zhang, J.; Liu, W.; Meng, Y.; Qin, D.; Yao, J.; Wang, W.; Chen, D. Pyroelectric infrared detector based on $LiTaO_3$ crystal with novelty nanostructured amorphous carbon film. In Proceedings of the IEEE 12th International Conference on Nano/Micro Engineered and Molecular Systems (NEMS), Los Angeles, CA, USA, 9–12 April 2017; pp. 623–626.
28. Hodgkinson, J.; Ralph, P.T. Optical gas sensing: A review. *Meas. Sci. Technol.* **2013**, *24*, 012004. [CrossRef]
29. Hodgkinson, J.; Smith, R. Non-dispersive infra-red (NDIR) measurement of carbon dioxide at 4.2 μm in a compact and optically efficient sensor. *Sens. Actuators B Chem.* **2013**, *186*, 580–588. [CrossRef]
30. Vincent, T.A.; Gardner, J.W. A low cost MEMS based NDIR system for the monitoring of carbon dioxide in breath analysis at ppm levels. *Sens. Actuators B Chem.* **2016**, *236*, 954–964. [CrossRef]
31. Vincent, T.A.; Urasinska-Wojcik, B. Development of a lowcost NDIR system for ppm detection of carbon dioxide in exhaled breath analysis. *Procedia Eng.* **2015**, *120*, 388–391. [CrossRef]
32. Mendes, L.B.; Ogink, N.W.; Edouard, N.; Van Dooren, H.J.; Tinôco, I.D.; Mosquera, J. NDIR gas sensor for spatial monitoring of carbon dioxide concentrations in naturally ventilated livestock buildings. *Sensors* **2015**, *15*, 11239–11257. [CrossRef]
33. Kwon, J.; Ahn, G.; Kim, G.; Kim, J.-C.; Kim, H. A study on NDIR-based CO_2 sensor to apply remote air quality monitoring system. In Proceedings of the ICCAS-SICE 2009—ICROS-SICE International Joint Conference, Fukuoka, Japan, 18–21 August 2009.
34. Popa, D.; Udrea, F. Towards integrated mid-infrared gas sensors. *Sensors* **2019**, *19*, 2076. [CrossRef]
35. Dinh, T.V.; Choi, I.Y. A review on non-dispersive infrared gas sensors: Improvement of sensor detection limit and interference correction. *Sens. Actuators B Chem.* **2016**, *231*, 529–538. [CrossRef]
36. Rothman, L.S.; Jacquemart, D. The HITRAN 2004 molecular spectroscopic database. *J. Quant. Spectrosc. Radiat. Transf.* **2005**, *96*, 139–204. [CrossRef]
37. Lee, R.; Kester, W. Complete gas sensor circuit using nondispersive infrared (NDIR). *Anal. Dialog.* **2016**, *50*, 10–18.

Disclaimer/Publisher's Note: The statements, opinions and data contained in all publications are solely those of the individual author(s) and contributor(s) and not of MDPI and/or the editor(s). MDPI and/or the editor(s) disclaim responsibility for any injury to people or property resulting from any ideas, methods, instructions or products referred to in the content.